DMD Fast Forward. Published on October 9, 2015 as DOI: 10.1124/dmd.115.066027
This article has not been copyedited and formatted. The final version may differ from this version.

DMD #66027

TITLE PAGE

Prediction of Drug Clearance and Drug-Drug Interactions in Microscale Cultures of Human Hepatocytes

Christine Lin, Julianne Shi, Amanda Moore, Salman R. Khetani

School of Biomedical Engineering (C.L., S.R.K.) and Department of Mechanical Engineering (S.R.K.), Colorado State University, Fort Collins, Colorado; Hepregen Corporation, Medford, Massachusetts (J.S., A.M.)

RUNNING TITLE PAGE

Running Title: Micropatterned co-cultures for drug clearance studies

CORRESPONDING AUTHOR CONTACT INFORMATION:

Salman R. Khetani, Ph.D.
Colorado State University
200 W. Lake St., 1374 Campus Delivery
Fort Collins, CO 80523-1374
Salman.Khetani@colostate.edu
Tel: 970-491-1302
Fax: 970-491-3827

Words in Abstract: 249
Words in Introduction: 749
Words in Discussion: 1500
Number of References: 35
Number of Figures: 6
Number of Tables: 3
Number of text pages: 39

ABBREVIATIONS:

CL_h, hepatic clearance
CL_{int}, intrinsic clearance
CYP450, cytochrome p450
DDI, drug-drug interactions
DMEs, drug metabolism enzymes
DMEM, Dulbecco's Modified Eagle Media
DMSO, dimethyl sulfoxide
FDA, Food and Drug Administration
F_u, fraction of unbound drug
LC-MS, liquid chromatography-mass spectrometry
Q, hepatic blood flow
$t_{1/2,}$ half-life
UGT, uridine 5'-diphospho-glucuronosyltransferase

DMD Fast Forward. Published on October 9, 2015 as DOI: 10.1124/dmd.115.066027
This article has not been copyedited and formatted. The final version may differ from this version.

ABSTRACT

Accurate prediction of *in vivo* hepatic drug clearance using *in vitro* assays is important to properly estimate clinical dosing regimens. Clearance of low turnover compounds is especially difficult to predict using short-lived suspensions of un-pooled primary human hepatocytes (PHHs) and functionally declining PHH monolayers. Micropatterned co-cultures (MPCCs) of PHHs and 3T3-J2 fibroblasts have been previously shown to display major liver functions for several weeks *in vitro*. In this study, we first characterized long-term activities of major cytochrome P450 (CYP) enzymes in MPCCs created from un-pooled cryopreserved PHH donors. Then, MPCCs were utilized to predict the clearance of 26 drugs that exhibit a wide range of turnover rates *in vivo* (0.05-19.5 mL/min/kg). MPCCs predicted 73%, 92% and 96% of drug clearance values for all tested drugs within 2-fold, 3-fold and 4-fold of *in vivo* values, respectively. There was good correlation (R^2=0.94, slope=1.05) of predictions between the two PHH donors. On the other hand, suspension hepatocytes and conventional monolayers created from the same donor had significantly reduced predictive capacity (i.e. 30-50% clearance values within 4-fold of *in vivo*), and were not able to metabolize several drugs. Finally, we modulated drug clearance in MPCCs by inducing or inhibiting CYPs. Rifampin-mediated CYP3A4 induction increased midazolam clearance by 73%, while CYP3A4 inhibition with ritonavir decreased midazolam clearance by 79%. Similarly, quinidine-mediated CYP2D6 inhibition reduced clearance of dextromethorphan and desipramine by 71% and 22%, respectively. In conclusion, MPCCs created using cryopreserved un-pooled PHHs can be utilized for drug clearance predictions and to model drug-drug interactions.

DMD Fast Forward. Published on October 9, 2015 as DOI: 10.1124/dmd.115.066027
This article has not been copyedited and formatted. The final version may differ from this version.

INTRODUCTION

Metabolism by the liver accounts for the overall clearance of ~70% of marketed drugs (Wienkers and Heath, 2005). Thus, accurate prediction of *in vivo* human hepatic clearance using preclinical models is important to set drug doses in the clinic (Ring *et al.*, 2011). Significant species-specific differences in liver pathways can lead to inaccuracies in the predictions of human drug clearance when using animals (Shih *et al.*, 1999). Therefore, *in vitro* human liver models are now increasingly utilized to predict human drug clearance (Di and Obach, 2015). While human liver microsomes are useful for evaluating cytochrome P450 (CYP)-mediated drug clearance in a high-throughput screening format, the lack of phase-II enzymes and membrane-bound transporters limits their utility for predicting clearances of different drug types. On the other hand, while retaining the complete architecture and cell types of the liver, liver slices are not amenable to high-throughput screening. Cancerous hepatic cell lines can be expanded cheaply and nearly indefinitely; however, they suffer from abnormal CYP levels and only represent single donors (Wilkening *et al.*, 2003). Thus, cryopreserved primary human hepatocytes (PHHs), which can be sourced from multiple donors, are ideal for on-demand assessment of drug disposition since they integrate all of the relevant metabolic pathways of the liver (Godoy *et al.*, 2013).

PHHs can be kept viable in suspension for 4-6h or plated in confluent monolayers on adsorbed collagen for a few days. For suspension PHHs, pooling can mitigate the large functional variability inherent across PHH donor lots. However, the limited incubation

time using suspension hepatocytes often does not allow low turnover drugs to deplete sufficiently to predict *in vivo* clearance (Brown *et al.*, 2007; Ring *et al.*, 2011). Low turnover drugs are increasingly being developed for one-pill-a-day dosing regimens, and often rank ordering of candidate compounds in a chemical series by clearance rates is necessary to progress with development. The relay method has addressed this limitation by transferring the drug-laden supernatant from 4h pooled PHH suspension incubations to freshly thawed PHHs to allow active enzymes to metabolize the drugs for prolonged times (~20h) (Di *et al.*, 2012). However, this method requires at least 5-fold more PHHs (10+ pooled donors) than a single incubation, thereby depleting a limited lot faster and necessitating screening and large-scale banking of newer pooled lots. Additionally, suspension hepatocytes don't properly polarize with appropriate localization of transporters to the apical and basolateral domains, which is limiting for predicting clearance of drugs that are transporter substrates. While plated monolayers prolong PHH viability for a few days and show polarized phenotype when overlaid with an extracellular matrix gel (Bi *et al.*, 2006), the CYP activities rapidly decline to <10% of levels observed in freshly isolated PHHs (Lecluyse, 2001; Khetani and Bhatia, 2008).

Organizing hepatocytes using engineering tools and co-culture with stromal cells can help maintain hepatic functions for prolonged times and at higher levels than possible with conventional monolayers, which has improved predictive capacities for drug studies (Khetani *et al.*, 2015). Khetani and Bhatia developed a micropatterned co-culture (MPCC) model in which PHHs are organized onto collagen-coated domains of empirically-optimized dimensions and subsequently surrounded by 3T3-J2 murine

embryonic fibroblasts (Khetani and Bhatia, 2008). Major hepatic functions (i.e. drug metabolism enzymes, transporters) are stable in MPCCs for ~4 weeks. Due to the reduced number of PHHs (~10% of confluent monolayers), MPCCs can be incubated for up to 7d without a medium change, which led to detection of a greater number of clinically-relevant metabolites than was possible with suspension PHHs (Wang *et al.*, 2010). Chan *et al.* also used the 7d drug incubations in MPCCs to predict clearance of low turnover compounds (Chan *et al.*, 2013). However, drugs with high clearance rates were not tested, nor was MPCC performance compared against suspension hepatocytes and plated monolayers using the same donor. Furthermore, it remains unclear whether MPCCs created using cryopreserved PHHs from multiple donors can maintain high levels of major CYPs for several weeks, which could allow initiation of drug incubation at different culture ages. Therefore, here we sought to determine levels and longevity of major CYP enzymes in MPCCs created from cryopreserved PHH donors (un-pooled) in a 96-well plate format. We then utilized MPCCs to predict clearance rates of 26 drugs with a wide range of *in vivo* turnover rates, and compared results for a subset of these drugs across MPCCs, suspension PHHs and plated monolayers created from the same donor. Finally, we assessed the effects of drug-mediated CYP modulation on drug clearance rates in order to mimic drug-drug interaction (DDI) scenarios.

MATERIALS AND METHODS

Culture of primary human hepatocytes

Cryopreserved PHHs were purchased from vendors permitted to sell products derived from human organs procured in the United States by federally designated Organ Procurement Organizations (BioreclamationIVT, Baltimore, MD; Triangle Research Laboratories, Research Triangle Park, NC; Life Technologies, Carlsbad, CA). Information (lot classifier, age, sex, ethnicity, cause of death, available medical history) on the PHH lots is provided in **Supplemental Table 1**. PHH vials were thawed at 37°C for 120s and diluted with 25 mL of pre-warmed KryoThaw I (SciKon, Chapel Hill, NC). The cell suspension was then spun at 50x*g* for 10 min, the supernatant was discarded, the cells were re-suspended in hepatocyte seeding medium, the formulation of which was described previously (Khetani *et al.*, 2013). Hepatocyte viability was assessed using trypan blue exclusion (typically 80-95%). Liver-derived non-parenchymal cells were consistently found to be less than 1% of all the cells.

MPCCs were created as previously described (Berger *et al.*, 2014). Briefly, adsorbed collagen was lithographically patterned in each well of a multi-well plate to create 500 µm diameter circular domains spaced 1200 µm apart, center-to-center. Hepatocytes selectively attached to the collagen domains leaving ~4,500 attached hepatocytes on ~13 collagen-coated islands within each well of a 96-well plate. 3T3-J2 murine embryonic fibroblasts were seeded 18 to 24h later in each well to create MPCCs.

DMD Fast Forward. Published on October 9, 2015 as DOI: 10.1124/dmd.115.066027
This article has not been copyedited and formatted. The final version may differ from this version.

Serum-supplemented culture medium, the formulation of which has been described previously (Ramsden *et al.*, 2014), was replaced on cultures every 2d (~64 µL/well).

To create suspension cultures, $5.6x10^4$ hepatocytes were dispensed into each well (32 µL serum-free culture medium per well) of an uncoated 96-well plate. To create conventional confluent monolayers, $5.6x10^4$ hepatocytes were seeded into each well (64 µL serum-supplemented culture medium per well) of a 96-well plate coated with rat-tail collagen type I as described previously (Khetani and Bhatia, 2008). Serum-free culture medium for both suspension cultures and conventional monolayers was composed of William's E base (Sigma-Aldrich, St. Louis, MO), 15 mM HEPES buffer (Corning Cellgro, Manassas, VA), 1% vol/vol ITS+ supplement (Corning Life Sciences, Tewksbury, MA), 1% vol/vol penicillin-streptomycin (Corning Cellgro), 100 nM dexamethasone (Sigma-Aldrich), 0.2% vol/vol amphotericin B (Life Technologies), and 0.01% vol/vol gentamycin (Life Technologies). Fetal bovine serum (Life Technologies) was added at 10% vol/vol for seeding conventional monolayers for 24h and then cultures were switched to the serum-free formulation above for drug dosing studies.

Hepatocyte functionality assays

Urea concentration in supernatants was assayed using a colorimetric endpoint assay utilizing diacetyl monoxime with acid and heat (Stanbio Labs, Boerne, TX). Albumin levels were measured using an enzyme-linked immunosorbent assay (MP Biomedicals, Irvine, CA) with horseradish peroxidase detection and 3,3',5,5'-tetramethylbenzidine

(TMB, Fitzgerald Industries, Concord, MA) as the substrate. CYP2C9 activity in cultures was measured using a luminescence-based assay (CYP2C9-glo, luciferin-H) by Promega (Madison, WI). Following incubation for 3h with the CYP2C9-glo substrate in serum-free dosing culture medium, culture supernatants were processed according to manufacturer instructions and luminescence was measured using a luminometer (BioTek, Winooski, VT). In addition, activities of major CYPs in MPCCs were assessed using substrates shown in **Supplemental Table 2**. Cultures were incubated with these substrates for 1h in serum-free dosing culture medium. Supernatants from cultures were frozen at -80°C prior to further analysis.

Drug dosing

MPCCs were allowed 7-9d to functionally stabilize and then dosed in serum-free culture medium with a set of 26 drugs (**Table 1**), ranging in known *in vivo* turnover rates between 0.05 mL/min/kg and 19.5 mL/min/kg. Conventional PHH monolayers were allowed 24h to acclimate before dosing in serum-free culture medium with a subset (10 total) of the drugs (**Table 2**). Suspension hepatocytes were dosed immediately after dispensing in wells with the same subset of drugs as those tested on conventional monolayers (**Table 3**). All drug solutions were prepared in serum-free culture medium at 1 µM and placed on the cells (64 µL total volume per well). MPCCs were incubated with drug solutions for up to 7d without a medium change; conventional monolayers were dosed for up to 4d; and, suspension cultures were dosed for up to 4h. Supernatants (50 µL) from representative wells (single time-point per well of a 96-well plate) were

collected at 6-7 time-points spread across the time series for each type of culture model. For MPCCs and conventional monolayers, removal of the supernatants was sufficient to stop the reaction with the cells. For suspension hepatocytes, however, mixing the cell suspension with 100 µL of acetonitrile was necessary to quench the reaction. All samples were immediately frozen at -80°C prior to further analysis.

For DDI studies, MPCCs stabilized for 7d were treated with serum-supplemented culture medium containing CYP inducer (12.5 µM rifampin for CYP3A4) for 3d or CYP inhibitor (0.5 µM ritonavir for CYP3A4 and 4 µM quinidine for CYP2D6) for 18h. Inducer and inhibitor concentrations were chosen based on preliminary experiments evaluating effects on the pertinent CYPs (data not shown). Then, cultures were dosed in serum-free culture medium with 1 µM of CYP substrates (midazolam for CYP3A4, and desipramine and dextromethorphan for CYP2D6) with or without CYP inducer/inhibitor. Control cultures were treated with dimethyl sulfoxide (DMSO, Corning Cellgro) alone (0.1% vol/vol) for the aforementioned time periods before dosing with CYP substrates. Sample collection was carried out as described above prior to further analysis.

Liquid Chromatography-Mass Spectrometry (LC-MS) Analysis

LC-MS analysis on culture supernatants (crashed with acetonitrile) was carried out by Integrated Analytical Solutions (IAS, Berkeley, CA). The amount of substrate metabolite or parent compound was measured using an Applied Biosystems/MDS Sciex API 3000 mass spectrometer (Foster City, CA) coupled to a Shimadzu VP System (Shimadzu,

Columbia, MD). The LC mobile phases consisted of: A) water containing 0.2% formic acid and B) methanol containing 0.2% formic acid. Samples were eluted through a Luna Mercury C8(2) column (2 x 30 mm; Phenomenex Inc., Torrance, CA), a Luna Mercury Hydro-RP column (2 x 3 mm), a Duragel G C18 column (2 x 10 mm; Peeke Scientific, Redwood City, CA), or a Titan 200 C18 column (2.1 x 30 mm; Sigma-Aldrich, St. Louis, MO). Solvent gradients from 0% (B) or 5% (B) to 95% (B) over the course of 1-2 minutes at flow rates of between 0.4 mL/min and 0.8 mL/min were used to elute the compounds from the columns. Injection volumes ranged from 2-100 µL for analysis.

Data analysis

The natural logarithm of the concentration of drug remaining in culture supernatants was first plotted against time of incubation. Further analysis of the data as described below was conducted only if the correlation coefficient of the linear fit to the natural log transformed data was greater than 0.8. If the correlation coefficient was less than 0.8, the data set was deemed not usable for prediction of clearance. The *in vitro* depletion half-lives of the drugs in culture supernatants were calculated by **equation 1**, where 'slope' was derived from the natural logarithm of the concentration of drug remaining plotted against time. For most of the compounds, the calculated half-life was within the maximal incubation time (i.e. no extrapolation) for both MPCCs and conventional monolayers, except for theophylline (both donors ~5 fold higher half-life than maximal incubation time), zolmatriptan (one of the two donors ~2 fold), and meloxicam (one of

the two donors ~2 fold). For suspension hepatocytes, half-life needed to be extrapolated beyond the incubation time for 6 of 10 drugs (~2-3 fold).

$$t_{1/2} = \frac{0.693}{slope}$$ Equation 1

Next, the *in vitro* drug half-lives were used to calculate the intrinsic clearance (CL_{int}) using scaling factors (**equation 2**), where 21 g of liver weight per 1 kg of body weight, and 120 x 10^6 hepatocytes per 1 g of human liver were utilized as standard parameters (Obach *et al.*, 1997). PHH numbers per well were 4,500 for MPCCs and 56,000 for suspension and conventional monolayers. All cultures had incubation volumes of 64 µL.

$$CL_{int} = \frac{Ln(2)}{t_{1/2}} \times \frac{liver\ weight}{standard\ body\ weight} \times \frac{incubation\ volume\ (mL)}{hepatocytes\ /well} \times \frac{hepatocytes}{gram\ of\ liver}$$ Equation 2

The hepatic clearance (CL_h) was calculated from CL_{int} using the well-stirred model (**equation 3**) with liver blood flow (Q) being 21 mL/min/kg and protein binding (f_u) set to 1 if no protein binding correction was made or to its respective known *in vivo* value (**Table 1**).

$$CL_h = \frac{Q \times f_u \times CL_{int}}{Q + (f_u \times CL_{int})}$$ Equation 3

Error bars on graphs represent standard errors of the means. Microsoft Excel and GraphPad Prism 5.0 (La Jolla, CA) were used for data analysis, while GraphPad Prism 5.0 was used for plotting data.

RESULTS

Long-term functional characterization of MPCCs

MPCCs were created in an industry-standard 96-well plate format using two cryopreserved PHH donors (lots: RTM and JNB). Prototypical hepatic morphology (polygonal shape, distinct nuclei and nucleoli, presence of bile canaliculi) was maintained for both donors in MPCCs for ~4 weeks (**Figure 1A and Supplemental Figure 1A**). As observed previously (Khetani and Bhatia, 2008), albumin secretion in MPCCs took ~7-9d to reach higher steady-state levels than in the first few days of culture (**Figure 1B and Supplemental Figure 1B**). Urea secretion, on the other hand, either remained stable from the very beginning of the culture period or showed some down-regulation initially followed by stabilization for the remainder of the time-series (**Figure 1C and Supplemental Figure 1C**). Although donor dependent differences in albumin and urea secretion (as well as other functional markers as described below) were observed, overall trends were similar.

Activities of CYP1A2, 2C9, 2D6, and 3A4 were measured in both donors over time by quantifying metabolites of prototypical substrates, whereas the activities of CYP2A6, 2B6, 2C8, 2C19, and 2E1 were measured only in donor RTM (**Supplemental Table 2**) due to limitations in number of vials available for donor JNB. While enzyme activities were detected for ~4 weeks in both donors, there were differences in both the kinetics and magnitude of time-course for specific CYP activities (**Figure 2 and Supplemental**

DMD Fast Forward. Published on October 9, 2015 as DOI: 10.1124/dmd.115.066027
This article has not been copyedited and formatted. The final version may differ from this version.

Figure 1). CYP1A2 activities in RTM- and JNB-MPCCs at ~4 weeks of culture were 90% and 72% of week 1 activities, respectively (**Figure 2A and Supplemental Figure 1D**). CYP2C9 activities in RTM- and JNB-MPCCs at ~4 weeks were 176% and 91% of week 1 activities, respectively (**Figure 2C and Supplemental Figure 1D**). CYP2D6 activities in RTM- and JNB-MPCCs at ~4 weeks were 73% and 85% of week 1 levels, respectively (**Figure 2D and Supplemental Figure 1E**). CYP3A4 activity in RTM at ~4 weeks was 131% of week 1 activity, while activity in JNB at 4 weeks had gradually declined to 58% of week 1 levels (**Figure 2E and Supplemental Figure 1E**). By ~4 weeks in RTM culture, CYP2A6 and CYP2B6 activities were down-regulated to 24% and 47% of week 1 levels, respectively. However, most of the decline occurred after 19d in culture (**Figures 2A-B**). CYP2C8 activity, on the other hand, was up-regulated by day 9 of culture to 658% of week 1 levels and then remained fairly stable until day 30 (**Figure 2B**). Use of CYP2C9-glo as a substrate showed similar relative stability as the measurement of 4-OH-tolbutamide in the same donor (**Figure 2C**). CYP2C19 activity was only stable for 15d followed by down-regulation to 22-33% of week 1 levels for the remainder of the time-series (**Figure 2D**). CYP2E1 activity at week 4 of culture declined to 12% of week 1 levels (**Figure 2E**). Nonetheless, activities of all major CYPs tested were detected out to at least 4 weeks in MPCCs created using both RTM and JNB donors. Lastly, we measured glucuronidation and sulfation (phase-II) activities in MPCCs created using both RTM and JNB donors (**Figure 2F and Supplemental Figure 1F**). By ~4 weeks in culture, RTM maintained phase-II activities to 90-116% of week 1 activities, while JNB at 4 weeks maintained activities to 77-105% of week 1 activities.

DMD Fast Forward. Published on October 9, 2015 as DOI: 10.1124/dmd.115.066027
This article has not been copyedited and formatted. The final version may differ from this version.

Drug clearance predictions in MPCCs

MPCCs were incubated for up to 7d with 26 drugs listed in **Table 1** (0.05-19.5 mL/min/kg *in vivo* clearance). Prototypical depletion of 3 drugs in MPCC supernatants is shown in **Supplemental Figure 2**. Drug clearance from *in vitro* MPCC data (and other models below) was predicted using the drug half-life, scaling parameters and well-stirred model as described in the 'methods' section. Predicted drug clearance rates in MPCCs with or without incorporation of protein binding into the analysis are shown in **Table 1**. Clearance data in 2 donors (JNB and RTM) was acquired for all drugs except timolol, imipramine and diclofenac, for which only a single donor was used due to PHH sourcing limitations. On average, with protein binding correction, MPCCs predicted 31%, 58% and 69% of the drug clearance values within 2-fold, 3-fold and 4-fold of *in vivo* clearance rates, respectively. When no protein binding correction was incorporated, MPCCs predicted on average 62%, 73% and 77% within 2-fold, 3-fold and 4-fold of *in vivo* clearance rates, respectively. We found that for compounds with *in vivo* reported clearance values less than or equal to ~1 mL/min/kg, correction for protein binding significantly improved MPCC predictive capacity, which is consistent with a previous study (Chan *et al.*, 2013). When utilizing a "mixed analysis" approach where correction for protein binding was only incorporated for compounds with reported clearance rates less than or equal to 1 mL/min/kg (low to very low turnover) and f_u=1 for all other compounds, MPCCs predicted 73%, 92% and 96% of the drug clearance values within 2-fold, 3-fold and 4-fold of *in vivo* clearance rates, respectively (**Table 1 and Figure 3**). Additionally, MPCCs were able to correctly rank order analog drugs based on predicted

DMD Fast Forward. Published on October 9, 2015 as DOI: 10.1124/dmd.115.066027
This article has not been copyedited and formatted. The final version may differ from this version.

clearance rates (sumatriptan/zolmatriptan, methylprednisolone/prednisolone and lorazepam/diazepam). Lastly, the predicted drug clearance values in MPCCs created from two donors for drugs with clearance rates greater than 5 mL/min/kg (**Figure 4A**) and less than 5 mL/min/kg (**Figure 4B**) were compared against each other using linear regression analysis. Both donors provided similar predictions of drug clearance rates across all drugs (average R^2=0.94, slope=1.05) despite the functional differences observed in figures 1 and 2, and supplemental figure 1.

Comparison of predicted drug clearance rates across different culture models

A subset of the drug set, 10 total drugs in particular across a wide range of *in vivo* turnover rates (0.19–19.5 mL/min/kg), were also tested in conventional PHH monolayers (**Table 2**) and suspension PHH cultures (**Table 3**) created from one of the PHH donors (RTM) utilized for MPCCs in Table 1. Prototypical depletion of 3 drugs in supernatants of conventional monolayers and suspension cultures is shown in **Supplemental Figures 3 and 4**, respectively. Conventional monolayers were useful for predicting clearance rates for 9 of 10 compounds, except for naproxen, which did not metabolize sufficiently in the monolayers to make a clearance prediction. Without protein binding correction, monolayers predicted 50%, 60% and 80% and with protein binding correction, 10%, 20% and 20% within 2-fold, 3-fold and 4-fold of *in vivo* clearance rates, respectively. When utilizing the “mixed analysis” approach as described above, monolayers predicted 40%, 40% and 50% of the clearance rates within 2-fold, 3-fold and 4-fold of *in vivo* clearance rates, respectively, which was in

contrast to the data obtained in MPCCs (80%, 100% and 100% within 2-fold, 3-fold and 4-fold, respectively, for the 10 drug subset). Most of the clearance rates obtained from monolayers were 12-86% lower than those predicted using MPCCs, with the exception of erythromycin (3% higher in monolayers relative to MPCCs) and theophylline (26% higher). For suspension cultures, 70% of the drugs with *in vivo* clearance rates of less than or equal to 6.1 mL/min/kg demonstrated little to no metabolism over the time course of 4h. For the 3 compounds that demonstrated metabolism in suspension cultures (verapamil, naloxone and timolol), clearance values were predicted within 3-fold of *in vivo* clearance values. Overall, 20%, 30% and 30% of the drug clearance were predicted within 2-fold, 3-fold and 4-fold of *in vivo* clearance rates, respectively, in suspension PHHs.

Effects of drug-drug interactions (DDI) on drug clearance rates

CYP3A4 activity was induced ~4 fold relative to vehicle control in MPCCs by a 3d treatment with rifampin, or CYP3A4 was inhibited down to ~4% relative to vehicle controls by an 18h treatment with ritonavir (data not shown). Inducing CYP3A4 levels by ~4 fold led to significantly more turnover of midazolam (56.4% depletion in vehicle control vs. 99.8% depletion in rifampin-treated cultures) over 24h of incubation (**Figure 5A**). On the other hand, incubation with ritonavir significantly inhibited midazolam turnover (8.2% depletion) relative to vehicle controls. When the turnover of midazolam over time was converted to predicted clearance rates, the vehicle control produced a rate within 2-fold of *in vivo* clearance (vehicle control: 10.7 mL/min/kg, *in vivo*: 8.7

DMD Fast Forward. Published on October 9, 2015 as DOI: 10.1124/dmd.115.066027
This article has not been copyedited and formatted. The final version may differ from this version.

mL/min/kg), while rates in both induced and inhibited cultures were outside the 2-fold window (induced: 18.5 mL/min/kg, inhibited: 2.3 mL/min/kg), albeit in opposite directions as expected (**Figure 5B**).

When we inhibited CYP2D6 in MPCCs using quinidine, turnover of dextromethorphan over a 96h incubation was significantly inhibited relative to vehicle control cultures (85% turnover in vehicle controls vs. 13.5% turnover in inhibited cultures) (**Figure 6A**). Predicted dextromethorphan clearance from the turnover data was within 2-fold of *in vivo* clearance in vehicle control cultures (vehicle control: 7.6 mL/min/kg, *in vivo*: 8.6 mL/min/kg), but outside 2-fold in inhibited cultures (2.2 mL/min/kg) (**Figure 6B**). On the other hand, effects of quinidine-mediated CYP2D6 inhibition were not as pronounced for desipramine turnover as for dextromethorphan (**Figure 6C-D**). In particular, 68% of desipramine was depleted over 48h in vehicle control cultures as opposed to 54% in inhibited cultures (**Figure 6C**). Such turnover corresponded to predicted desipramine clearance rates within 2-fold of *in vivo* clearance for both vehicle control and quinidine-inhibited cultures (vehicle control: 8.5 mL/min/kg, quinidine-inhibited: 6.6 mL/min/kg, *in vivo*: 10.3 mL/min/kg) (**Figure 6D**).

DISCUSSION

Prediction of *in vivo* human drug clearance using *in vitro* hepatic clearance data can help identify compounds with poor pharmacokinetic characteristics. An ideal hepatocyte culture platform for such purposes uses as few limited PHHs as possible in a reproducible/miniaturized format; maintains high levels of drug metabolism enzymes (DMEs) with proper hepatocyte polarity to allow incubations with drugs that interact with multiple pathways; is compatible with multiple cryopreserved PHH donors for on-demand screening; and, can be used to predict clearance of compounds with a wide range of turnover rates, including slowly metabolized compounds. Additionally, the ability to interrogate effects of drug incubations on PHH enzyme levels and subsequently victim drug disposition is important for modeling clinical DDIs (Khetani *et al.*, 2015). Towards approximating such features, we show that MPCCs created in a 96-well plate format display high levels of CYP and phase-II activities for ~4 weeks. Such activities coupled with the ability to dose drugs for 7d without a medium change led to better overall prediction of drug clearance rates than with suspension cultures or conventional monolayers created from the same donor. Finally, modulating CYP activities via perpetrator drugs altered the clearance of victim drugs in MPCCs.

We quantified albumin secretion, urea synthesis and enzyme activities over several weeks in MPCCs created from two cryopreserved PHH donors. The fibroblasts used in MPCCs do not metabolize drugs that primarily undergo hepatic metabolism (Khetani and Bhatia, 2008; Chan *et al.*, 2013). Albumin and urea secretion rates in MPCCs were

relatively stable across both donors for 3-4 weeks. CYP1A2, 2C9, 2D6, glucuronidation/sulfation activities were relatively stable between 1 and 4 weeks of culture across both donors; however, CYP3A4 declined by ~40% in one donor. We also measured the activities of CYP2A6, 2B6, 2C8, 2C19 and 2E1 in a single donor. CYP2A6 and 2B6 were relatively stable for ~3 weeks; 2C19 activity was relatively stable for ~2 weeks; and, CYP2E1 levels showed a decline between 1 and 4 weeks of culture. Nonetheless, activities of all major enzymes tested were detected for ~4 weeks in MPCCs with good stability for 2-3 weeks for most CYPs. Culture medium formulations that can improve the stability of all major CYPs in MPCCs for at least 4 weeks should prove useful for drug dosing at later time points.

The 26 drugs chosen span a larger range of *in vivo* turnover rates (0.05-19.5 mL/min/kg) than previously tested in MPCCs (Chan *et al.*, 2013). These drugs can undergo metabolism via CYPs (i.e. tolbutamide, diclofenac) and phase II enzymes (naloxone, diazepam), while some are transporter substrates (i.e. triprolidine, desipramine) (McGinnity *et al.*, 2004; Koepsell *et al.*, 2007). The well-stirred model was used to predict clearance from drug depletion in supernatants, an approach well suited for screening large numbers of compounds. Marginal differences have been observed across well-stirred, parallel-tube and dispersion models for clearance prediction, except for very high turnover compounds (Hallifax *et al.*, 2010). However, the well-stirred model produced good predictions for the high turnover compounds here. On average across two donors, MPCCs predicted 19 of 26 compounds (73%) within 2-fold of the known *in vivo* clearance rates, 24 of 26 compounds (92%) within 3-fold, and 25 of 26 compounds

DMD Fast Forward. Published on October 9, 2015 as DOI: 10.1124/dmd.115.066027
This article has not been copyedited and formatted. The final version may differ from this version.

(96%) within 4-fold, with meloxicam's predicted clearance rate at a 6-fold deviation. In another study with MPCCs and in another engineered liver platform, meloxicam was under-predicted and its turnover was highly dependent on the donor (Dash *et al.*, 2009; Chan *et al.*, 2013).

The accuracy of predicted clearance rates for high and medium turnover compounds was improved when not incorporating plasma protein binding, as also observed previously (Hallifax *et al.*, 2010; Ring *et al.*, 2011). On the other hand, MPCCs metabolized low turnover drugs (less than or equal to 1 mL/min/kg) significantly faster in the serum-free medium than *in vivo*, and thus use of reported f_u values significantly improved the accuracy of clearance predictions, as also observed previously (Blanchard *et al.*, 2005; Smith *et al.*, 2012). While the mechanism is not known, others have speculated that since slowly metabolized compounds have more time to bind to proteins *in vivo* than higher turnover compounds, the unbound fraction available for metabolism for slowly metabolized compounds may be lower than for higher turnover compounds (Atkinson and Kushner, 1979). Therefore, incorporation of protein binding correction in the analysis for low turnover compounds becomes important for more accurate clearance predictions. It is possible that inclusion of human albumin, alpha-1 acid glycoprotein and lipoproteins in culture medium at concentrations found in human blood may allow a more consistent analysis scheme for the entire range of drug turnover rates (Chao *et al.*, 2009).

The predicted drug clearance rates across two PHH donors used in MPCCs were strongly correlated (average R^2=0.94, slope=1.05) despite differences in CYP activities. Furthermore, in comparison to another study that tested 7 of 26 compounds used here with the same two donors in MPCCs (Chan *et al.*, 2013), we found good agreement with the rank ordering of drugs by their predicted clearance rates, thereby showing the reproducibility of the platform. With their use of individual PHH donors and ~40-50% fewer cells for seeding as compared to suspension and conventional confluent cultures, MPCCs can be used with limited donor lots for a larger number (~2-3 fold) of screening studies. Pooled plateable PHH lots could provide an "average" human response in plated culture formats; however, plating efficiencies need to be uniform across the various PHH donor lots to ensure that monolayers are composed of similar numbers of each donor's PHHs. Nonetheless, individual PHH lots with specific polymorphisms can provide useful information on population-specific differences in drug clearance.

Suspension PHHs, created from the same donor as that used in MPCCs, did not sufficiently deplete medium and low turnover drugs (7 of 10) within 4h to allow prediction of clearance rates, while clearance rates of higher turnover drugs were predicted within 2-3 fold of *in vivo* levels. Thus, while single donors can be used in MPCCs, carefully selected 10+ donor pooled lots along with the relay method are necessary to use suspension PHHs for prediction of medium and low turnover compounds (Di *et al.*, 2012). On the other hand, conventional PHH monolayers predicted the clearance rates for 9 of 10 drugs. Even though conventional monolayers display a rapid decline in functionality within the first 4-24h (Khetani *et al.*, 2015),

DMD Fast Forward. Published on October 9, 2015 as DOI: 10.1124/dmd.115.066027
This article has not been copyedited and formatted. The final version may differ from this version.

continued metabolism of some low turnover compounds (i.e. diazepam) was observed over 4d . Naproxen, however, did not turnover in conventional monolayers even after 4d of incubation even though it was depleted within 3d in MPCCs, which contained ~10-fold fewer PHHs. Overall, conventional monolayers predicted 40%, 40% and 50% of the compounds within 2-, 3- and 4-fold of *in vivo* turnover rates, respectively, whereas MPCCs predicted 80% and 100% within 2- and 3-fold, respectively. Furthermore, conventional monolayers predicted lower clearance rates than in MPCCs for 8 of 10 drugs, likely due to the lower enzyme activity per cell in conventional monolayers (Khetani and Bhatia, 2008).

The short lifetime (<7d) of conventional PHH monolayers coupled with a significant decline in CYP activities limits their utility in evaluating effects of CYP modulation on drug disposition, especially for those CYPs (i.e. 2D6) that are not as abundant as 3A4 (Khetani *et al.*, 2015). Here, we hypothesized that the greater longevity and higher functionality of MPCCs could help mitigate such a limitation. Inducing CYP3A4 in MPCCs via rifampin for 3d led to a ~73% increase in subsequent midazolam clearance, while inhibiting CYP3A4 via ritonavir for 18h led to a ~79% decrease in midazolam clearance relative to vehicle controls. The ~1.7 fold increase in midazolam clearance in MPCCs with rifampin pre-treatment is in line with the ~2 fold increase observed in the clinic, albeit live patients were pre-treated with rifampin for 7d (Gorski *et al.*, 2003). Furthermore, our use of serum with inducers in MPCC culture medium coupled with higher baseline CYP activities typically leads to lower fold induction values (2-8 fold) than can be observed with declining conventional monolayers incubated with inducers

in serum-free medium (up to 80-100 fold)(Rae *et al.*, 2001; Hariparsad *et al.*, 2004; Williamson *et al.*, 2013). Inhibition of CYP2D6 via quinidine led to ~71% and ~22% reduction in clearance of dextromethorphan and desipramine, respectively, relative to controls. Such a difference across the compounds highlights the need for evaluating the effects of DDI on drug clearance *in vitro*.

Incorporation of liver stromal cells in MPCCs may allow prediction of drug clearance rates under disease perturbations such as fibrosis and inflammation (Nguyen *et al.*, 2015). Furthermore, miniaturization into a 384-well format should enable higher-throughput screening in MPCCs. In conclusion, we show that MPCCs with cryopreserved PHHs can predict the clearance rates of drugs with a wide range of *in vivo* turnover rates, including slowly metabolized drugs. The accuracy of drug clearance prediction in MPCCs was significantly better than that observed in suspension and conventional monolayers created from the same donor. Furthermore, the longevity of MPCCs allowed evaluation of the effects of DDI on drug clearance, which should prove useful for better modeling clinical scenarios.

ACKNOWLEDGEMENTS

We are grateful to Dustin Berger and Brenton Ware for assistance with cell culture.

AUTHORSHIP CONTRIBUTIONS

Participated in research design: Lin, Shi, Moore, and Khetani.

Conducted experiments: Lin, Shi, and Moore.

Contributed new reagents or analytic tools:

Performed data analysis: Lin and Khetani.

Wrote or contributed to the writing of the manuscript: Lin and Khetani.

REFERENCES

Atkinson AJ, and Kushner W (1979) Clinical pharmacokinetics. *Annu Rev Pharmacol Toxicol* **19**:105–127.

Berger DR, Ware BR, Davidson MD, Allsup SR, and Khetani SR (2014) Enhancing the functional maturity of iPSC-derived human hepatocytes via controlled presentation of cell-cell interactions in vitro. *Hepatology* **61**:1370-1381.

Bi Y-A, Kazolias D, and Duignan DB (2006) Use of cryopreserved human hepatocytes in sandwich culture to measure hepatobiliary transport. *Drug Metabolism and Disposition* **34**:1658–1665.

Blanchard N, Alexandre E, Abadie C, Lavé T, Heyd B, Mantion G, Jaeck D, Richert L, and Coassolo P (2005) Comparison of clearance predictions using primary cultures and suspensions of human hepatocytes. *Xenobiotica* **35**:1–15.

Brown HS, Griffin M, and Houston JB (2007) Evaluation of cryopreserved human hepatocytes as an alternative in vitro system to microsomes for the prediction of metabolic clearance. *Drug Metabolism and Disposition* **35**:293–301.

Brunton L, Chabner B, and Knollman B (2011) *Goodman and Gilman's The Pharmacological Basis of Therapeutics, Twelfth Edition*, McGraw-Hill Professional.

Chan TS, Yu H, Moore A, Khetani SR, Khetani SR, and Tweedie D (2013) Meeting the Challenge of Predicting Hepatic Clearance of Compounds Slowly Metabolized by Cytochrome P450 Using a Novel Hepatocyte Model, HepatoPacTM. *Drug Metab Dispos* **41**:2024–2032.

Chao P, Chao P, Barminko J, Barminko J, Novik E, Novik E, Han Y, Han Y, Maguire T, Maguire T, Cheng KC, and Cheng KC (2009) Prediction of human hepatic clearance using an in vitro plated hepatocyte clearance model. *Drug Metab Lett* **3**:296–307.

Dash A, Inman W, Hoffmaster K, Sevidal S, Kelly J, Obach RS, Griffith LG, and Tannenbaum SR (2009) Liver tissue engineering in the evaluation of drug safety. *Expert Opin Drug Metab Toxicol* **5**:1159–1174.

Di L, and Obach RS (2015) Addressing the challenges of low clearance in drug research. *AAPS J* **17**:352–357.

Di L, Hsu IC, Trapa P, Tokiwa T, Obach RS, Bennett W, Atkinson K, Metcalf RA, Bi Y-A, Welsh JA, Wolford AC, Sun T, Tan B, Harris CC, McDonald TS, Lai Y, and Tremaine LM (2012) A novel relay method for determining low-clearance values. *Drug Metab Dispos* **40**:1860–1865.

Godoy P, Hewitt NJ, Albrecht U, Andersen ME, Ansari N, Bhattacharya S, Bode JG, Bolleyn J, Borner C, Böttger J, Braeuning A, Budinsky RA, Burkhardt B, Cameron NR, Camussi G, Cho C-S, Choi Y-J, Craig Rowlands J, Dahmen U, Damm G,

Dirsch O, Donato MT, Dong J, Dooley S, Drasdo D, Eakins R, Ferreira KS, Fonsato V, Fraczek J, Gebhardt R, Gibson A, Glanemann M, Goldring CEP, Gómez-Lechón MJ, Groothuis GMM, Gustavsson L, Guyot C, Hallifax D, Hammad S, Hayward A, Häussinger D, Hellerbrand C, Hewitt P, Hoehme S, Holzhütter H-G, Houston JB, Hrach J, Ito K, Jaeschke H, Keitel V, Kelm JM, Kevin Park B, Kordes C, Kullak-Ublick GA, LeCluyse EL, Lu P, Luebke-Wheeler J, Lutz A, Maltman DJ, Matz-Soja M, McMullen P, Merfort I, Messner S, Meyer C, Mwinyi J, Naisbitt DJ, Nussler AK, Olinga P, Pampaloni F, Pi J, Pluta L, Przyborski SA, Ramachandran A, Rogiers V, Rowe C, Schelcher C, Schmich K, Schwarz M, Singh B, Stelzer EHK, Stieger B, Stöber R, Sugiyama Y, Tetta C, Thasler WE, Vanhaecke T, Vinken M, Weiss TS, Widera A, Woods CG, Xu JJ, Yarborough KM, and Hengstler JG (2013) Recent advances in 2D and 3D in vitro systems using primary hepatocytes, alternative hepatocyte sources and non-parenchymal liver cells and their use in investigating mechanisms of hepatotoxicity, cell signaling and ADME. *Arch Toxicol* **87**:1315–1530.

Gorski JC, Vannaprasaht S, Hamman MA, Ambrosius WT, Bruce MA, Haehner-Daniels B, and Hall SD (2003) The effect of age, sex, and rifampin administration on intestinal and hepatic cytochrome P450 3A activity. *Clin Pharmacol Ther* **74**:275–287.

Hallifax D, Foster JA, and Houston JB (2010) Prediction of human metabolic clearance from in vitro systems: retrospective analysis and prospective view. *Pharm Res* **27**:2150–2161.

Hariparsad N, Nallani SC, Sane RS, Buckley DJ, Buckley AR, and Desai PB (2004) Induction of CYP3A4 by efavirenz in primary human hepatocytes: comparison with rifampin and phenobarbital. *J Clin Pharmacol* **44**:1273–1281.

Khetani SR, and Bhatia SN (2008) Microscale culture of human liver cells for drug development. *Nat Biotechnol* **26**:120–126.

Khetani SR, Berger DR, Ballinger KR, Davidson MD, Lin C, and Ware BR (2015) Microengineered Liver Tissues for Drug Testing. *J Lab Autom* **20:** 216-250.

Khetani SR, Kanchagar C, Ukairo O, Krzyzewski S, Moore A, Shi J, Aoyama S, Aleo M, and Will Y (2013) Use of micropatterned cocultures to detect compounds that cause drug-induced liver injury in humans. *Toxicol Sci* **132**:107–117.

Koepsell H, Lips K, and Volk C (2007) Polyspecific organic cation transporters: structure, function, physiological roles, and biopharmaceutical implications. *Pharm Res* **24**:1227–1251.

Lau YY, Sapidou E, Cui X, White RE, and Cheng KC (2002) Development of a novel in vitro model to predict hepatic clearance using fresh, cryopreserved, and sandwich-cultured hepatocytes. *Drug Metabolism and Disposition* **30**:1446–1454.

Lecluyse EL (2001) Human hepatocyte culture systems for the in vitro evaluation of cytochrome P450 expression and regulation. *European journal of pharmaceutical sciences : official journal of the European Federation for Pharmaceutical Sciences* **13**:343–368.

McGinnity DF, Soars MG, Urbanowicz RA, and Riley RJ (2004) Evaluation of fresh and cryopreserved hepatocytes as in vitro drug metabolism tools for the prediction of metabolic clearance. *Drug Metabolism and Disposition* **32**:1247–1253.

Nguyen TV, Ukairo O, Khetani SR, McVay M, Kanchagar C, Seghezzi W, Ayanoglu G, Irrechukwu O, and Evers R (2015) Establishment of a Hepatocyte-Kupffer Cell Co-Culture Model for Assessment of Proinflammatory Cytokine Effects on Metabolizing Enzymes and Drug Transporters. *Drug Metab Dispos* **43**:774-785.

Obach RS (1999) Prediction of human clearance of twenty-nine drugs from hepatic microsomal intrinsic clearance data: An examination of in vitro half-life approach and nonspecific binding to microsomes. *Drug Metabolism and Disposition* **27**:1350–1359.

Obach RS, Baxter JG, Liston TE, Silber BM, Jones BC, MacIntyre F, Rance DJ, and Wastall P (1997) The prediction of human pharmacokinetic parameters from preclinical and in vitro metabolism data. *J Pharmacol Exp Ther* **283**:46–58.

Obach RS, Lombardo F, and Waters NJ (2008) Trend Analysis of a Database of Intravenous Pharmacokinetic Parameters in Humans for 670 Drug Compounds. *Drug Metabolism and Disposition* **36**:1385–1405.

Rae JM, Johnson MD, Lippman ME, and Flockhart DA (2001) Rifampin is a selective, pleiotropic inducer of drug metabolism genes in human hepatocytes: studies with cDNA and oligonucleotide expression arrays. *J Pharmacol Exp Ther* **299**:849–857.

Ramsden D, Tweedie DJ, Chan TS, and Tracy TS (2014) Altered CYP2C9 activity following modulation of CYP3A4 levels in human hepatocytes: an example of protein-protein interactions. *Drug Metab Dispos* **42**:1940–1946.

Ring BJ, Chien JY, Adkison KK, Jones HM, Rowland M, Jones RD, Yates JWT, Ku MS, Gibson CR, He H, Vuppugalla R, Marathe P, Fischer V, Dutta S, Sinha VK, Björnsson T, Lavé T, and Poulin P (2011) PhRMA CPCDC initiative on predictive models of human pharmacokinetics, part 3: comparative assessement of prediction methods of human clearance. *J Pharm Sci* **100**:4090–4110.

Shih H, Pickwell GV, Guenette DK, Bilir B, and Quattrochi LC (1999) Species differences in hepatocyte induction of CYP1A1 and CYP1A2 by omeprazole. *Human & experimental toxicology* **18**:95–105.

Smith CM, Nolan CK, Edwards MA, Hatfield JB, Stewart TW, Ferguson SS, LeCluyse EL, and Sahi J (2012) A comprehensive evaluation of metabolic activity and intrinsic clearance in suspensions and monolayer cultures of cryopreserved primary human hepatocytes. *J Pharm Sci* **101**:3989–4002.

Wang WW, Khetani SR, Krzyzewski S, Duignan DB, and Obach RS (2010) Assessment of a Micropatterned Hepatocyte Coculture System to Generate Major Human Excretory and Circulating Drug Metabolites. *Drug Metab Dispos* **38**:1900–1905.

Wienkers LC, and Heath TG (2005) Predicting in vivo drug interactions from in vitro drug discovery data. *Nat Rev Drug Discov* **4**:825–833.

Wilkening S, Stahl F, and Bader A (2003) Comparison of primary human hepatocytes and hepatoma cell line Hepg2 with regard to their biotransformation properties. *Drug Metab Dispos* **31**:1035–1042.

Williamson B, Dooley KE, Zhang Y, Back DJ, and Owen A (2013) Induction of influx and efflux transporters and cytochrome P450 3A4 in primary human hepatocytes by rifampin, rifabutin, and rifapentine. *Antimicrob Agents Chemother* **57**:6366–6369.

Footnotes

Funding was provided by the National Science Foundation (CAREER Award CBET 1351909 to S.R.K.) and Colorado State University.

S.R.K. is an equity holder in Hepregen Corporation, which has exclusively licensed the MPCC technology from M.I.T. for drug development applications.

DMD Fast Forward. Published on October 9, 2015 as DOI: 10.1124/dmd.115.066027
This article has not been copyedited and formatted. The final version may differ from this version.

LEGENDS FOR FIGURES

Figure 1. Morphology and functional characterization of MPCCs created using cryopreserved PHHs. (A) Phase contrast micrographs of patterned PHHs (donor: RTM) prior to seeding of the 3T3-J2 murine embryonic fibroblasts (left) and 8 days in co-culture (right). Cultures showed similar hepatic morphology for at least 4 weeks (not shown). (B) Albumin secretion rates in MPCCs over time in culture. (C) Urea secretion rates in MPCCs over time in culture. Data in each graph was fit to a sigmoidal curve using GraphPad Prism 5.0 software. Error bars represent standard errors of the means (n=3).

Figure 2. CYP activities in MPCCs created using cryopreserved PHHs. Quantification of CYP-generated metabolites from MPCCs (donor: RTM). *CYP, probe substrate, metabolite measured:* (A) 1A2, phenacetin, acetaminophen; 2A6, coumarin, 7-OH-coumarin; (B) 2B6, bupropion, OH-bupropion; 2C8, paclitaxel, 6α-OH-paclitaxel; (C) 2C9, tolbutamide, 4-OH-tolbutamide; 2C9, 2C9-glo, luciferin; (D) 2C19, S-mephenytoin, 4-OH-S-mephenytoin; 2D6, dextromethorphan, dextrorphan; (E) 2E1, chlorzoxazone, 6-OH-chlorzoxazone; 3A4, testosterone, 6β-OH-testosterone. (F) Production rates of glucuronide and sulfate metabolites of 7-hydroxycoumarin from MPCCs. Error bars represent standard errors of the means (n=3).

Figure 3. Correlation between drug clearance rates predicted in MPCCs and rates reported *in vivo*. The predicted clearance rates shown here are averaged from data

obtained using two PHH donors in MPCCs for all drugs except timolol, imipramine and diclofenac, for which only a single donor was used (see table 1). PHH donor 1 was RTM while PHH donor 2 was either JNB or Hu4163. Open circles indicate predictions within 2-fold of *in vivo* levels (dashed lines); open squares indicate predictions within 3-fold (dotted lines); crosses indicate predictions within 4-fold; and X's indicate predictions greater than 4-fold (meloxicam). The solid line represents a perfect correlation. (A) Correlation analysis for all 26 compounds tested in this study. (B) Correlation analysis for a subset of compounds (*in vivo* reported clearance rates less than or equal to 1 mL/min/kg), for which data appears in the solid box marked in the graph of panel A.

Figure 4. Correlation between drug clearance rates predicted in MPCCs created from two PHH donors. PHH donor 1 was RTM while PHH donor 2 was either JNB or Hu4163. (A) Comparison between two donors for compounds with reported *in vivo* clearance rates greater than 5 mL/min/kg. (B) Comparison between two donors for compounds with reported *in vivo* clearance rates less than 5 mL/min/kg.

Figure 5. CYP3A4 drug-drug interaction studies in MPCCs. MPCCs created using PHH donor Hum4011 were stabilized for 7 days prior to being treated with vehicle only (dimethyl sulfoxide), rifampin (3A4 inducer, 12.5 μM) for 3 days, or ritonavir (3A4 inhibitor, 0.5 μM) for 18 hours. The cultures were then dosed with 1 μM midazolam (3A4 substrate). (A) Midazolam depletion in the supernatants of cultures treated with the aforementioned compounds. The arrow indicates a low amount of midazolam detected (0.23% +/- 0.07% relative to t=0) in supernatants of rifampin-treated MPCCs at 1440

min of incubation. (B) Predicted midazolam clearance rates from MPCCs treated with the aforementioned compounds. Dashed line indicates the reported *in vivo* midazolam clearance rate of 8.7 mL/min/kg. Similar trends were observed with a second donor, EJW (data not shown).

Figure 6. CYP2D6 drug-drug interaction studies in MPCCs. MPCCs created using PHH donor Hum4011 were stabilized for 7 days prior to being treated with vehicle only (dimethyl sulfoxide) or quinidine (2D6 inhibitor, 4 µM) for 18 hours. The cultures were then dosed with 1 µM desipramine or dextromethorphan (2D6 substrates). (A) Dextromethorphan depletion in the supernatants of cultures treated with the aforementioned compounds. (B) Predicted dextromethorphan clearance rates from MPCCs treated with the aforementioned compounds. Dashed line indicates the reported *in vivo* dextromethorphan clearance rate of 8.6 mL/min/kg. (C) Desipramine depletion in the supernatants of cultures treated with the aforementioned compounds. (D) Predicted desipramine clearance rates from MPCCs treated with the aforementioned compounds. Dashed line indicates the reported *in vivo* desipramine clearance rate of 10.3 mL/min/kg. Similar trends were observed with a second donor, EJW (data not shown).

TABLES

In Vivo Observed Pharmacokinetic Parameters				Predicted Clearance (mL/min/kg) in MPCCs					
				f_u = reported literature values			f_u = 1		
Compound Name	**Known Routes of Metabolism**	***In Vivo* CL (mL/min/kg)**	**f_u**	**Donor 1**	**Donor 2**	**Average**	**Donor 1**	**Donor 2**	**Average**
Verapamil	CYP3A4, 2C9	19.5	0.10	6.79	6.86	6.83	17.36	17.41	17.39
Sumatriptan		19	0.83	12.36	13.74	13.05	13.29	14.60	13.95
Naloxone	UGT2B7	18	0.54	14.45	14.52	14.49	16.87	16.92	16.90
Propranolol	CYP2D6, 1A2	15.7	0.13	6.70	4.95	5.83	16.44	14.77	15.61
Metoprolol*	CYP2D6	13	0.88	3.80	5.76	4.78	4.29	5.37	4.83
Triprolidine*		13	0.50	3.30	7.78	5.54	5.70	11.35	8.52
Desipramine*	CYP2D6, 1A2; UGT	10.3	0.16	2.25	2.39	2.32	8.99	9.34	9.16
Timolol	CYP2D6	10.1	0.90	5.39	N/A	5.39	5.82	N/A	5.82
Dextromethorphan	CYP2D6, 3A4, 1A2, 2C19	8.6	0.50	10.66	11.39	11.03	14.14	14.77	14.46
Omeprazole	CYP2C19, 3A4	8.4	0.05	2.53	2.47	2.50	15.38	15.26	15.32
Imipramine*	CYP2D6, 1A2, 2C19, 3A4; UGT1A4	8	0.10	N/A	2.06	2.06	N/A	10.93	10.93
Diclofenac	CYP2C9	7.6	0.01	0.08	N/A	0.08	8.90	N/A	8.90
Zolmitriptan	CYP1A2	6.7	0.75	1.94	3.01	2.48	2.51	3.83	3.17
Methylprednisolone	CYP3A4	6.1	0.23	4.67	6.57	5.62	11.64	13.95	12.80
Erythromycin	CYP3A4	5.6	0.10	0.71	1.06	0.89	5.44	7.30	6.37
Ziprasidone	CYP3A4	5.1	0.00	0.10	0.10	0.10	16.66	16.63	16.65
Betaxolol*		4.8	0.40	0.83	0.21	0.52	4.20	3.15	3.67
Prednisolone*	CYP3A4	2.9	0.25	0.68	0.59	0.64	3.36	3.08	3.22
Furosemide*		1.7	0.01	0.03	0.04	0.04	2.51	2.74	2.63
Theophylline	CYP1A2	1.1	0.41	0.34	0.26	0.30	0.81	0.62	0.72
Lorazepam	UGT	1	0.09	0.46	0.43	0.45	4.15	3.97	4.06
Diazepam	CYP2C19, 1A2, 3A4	0.53	0.02	0.21	0.22	0.22	6.30	6.69	6.50

DMD Fast Forward. Published on October 9, 2015 as DOI: 10.1124/dmd.115.066027
This article has not been copyedited and formatted. The final version may differ from this version.

Tolbutamide	CYP2C9, 2C19	0.38	0.05	0.21	0.40	0.31	3.49	5.84	4.67
Naproxen	CYP2C9, 1A2	0.19	0.01	0.18	0.49	0.34	9.75	14.78	12.27
Meloxicam	CYP2C9, 3A4	0.12	0.01	0.01	0.03	0.02	1.38	3.98	2.68
Warfarin*	CYP2C9, 3A4	0.05	0.02	0.04	0.02	0.03	1.85	1.02	1.44
		Within 2-fold		32%	25%	31%	60%	63%	62%
		Within 3-fold		48%	58%	58%	68%	71%	73%
		Within 4-fold		64%	71%	69%	76%	79%	77%

Table 1. Predicted clearance rates in MPCCs for 26 drugs. Donor 1 is the RTM lot. Asterisks next to compound names indicate that Donor 2 was Hu4163, rather than JNB. N/A indicates data are “not available” due to cell sourcing limitations. The *in vivo* PK parameters were compiled from several sources including: (Obach, 1999; Lau *et al.*, 2002; McGinnity *et al.*, 2004; Brown *et al.*, 2007; Obach *et al.*, 2008; Brunton *et al.*, 2011; Chan *et al.*, 2013).

***In Vivo* Observed Pharmacokinetic Parameter Values**			**Predicted Clearance (mL/min/kg)**			
			f_u = reported literature values		**f_u = 1**	
Compound Name	***In Vivo* CL (mL/min/kg)**	**f_u**	**MPCCs**	**Conventional Monolayer**	**MPCCs**	**Conventional Monolayer**
Verapamil	19.5	0.10	6.79	0.8	17.36	5.98
Naloxone	18	0.54	14.45	11.98	16.87	14.93
Timolol	10.1	0.90	5.39	0.95	5.82	1.05
Methylprednisolone	6.1	0.23	4.67	0.91	11.64	3.46
Erythromycin	5.6	0.10	0.71	0.73	5.44	5.59
Theophylline	1.1	0.41	0.34	0.43	0.81	1.02
Lorazepam	1	0.09	0.46	0.11	4.15	1.13
Diazepam	0.53	0.02	0.21	0.03	6.3	1.27
Tolbutamide	0.38	0.05	0.21	0.06	3.49	1.19
Naproxen	0.19	0.01	0.18	-	9.75	-
Within 2-fold			50%	10%	60%	50%
Within 3-fold			80%	20%	60%	60%
Within 4-fold			90%	20%	60%	80%

Table 2. Predicted drug clearance rates in MPCCs as compared to conventional confluent monolayers created using the same donor (RTM). MPCCs were stabilized for 7 days prior to dosing with drugs for up to 7 days, while conventional monolayers were stabilized for 1 day prior to dosing with drugs for up to 4 days. The '-' indicates that the drug did not turnover sufficiently in the model system to predict a clearance rate.

DMD Fast Forward. Published on October 9, 2015 as DOI: 10.1124/dmd.115.066027
This article has not been copyedited and formatted. The final version may differ from this version.

***In Vivo* Observed Pharmacokinetic Parameter Values**			**Predicted Clearance (mL/min/kg)**			
			f_u = reported literature values		**f_u = 1**	
Compound Name	***In Vivo* CL (mL/min/kg)**	**f_u**	**MPCCs**	**Suspension**	**MPCCs**	**Suspension**
Verapamil	19.5	0.10	6.79	1.23	17.36	8.03
Naloxone	18	0.54	14.45	11.12	16.87	14.19
Timolol	10.1	0.90	5.39	4.66	5.82	5.06
Methylprednisolone	6.1	0.23	4.67	-	11.64	-
Erythromycin	5.6	0.10	0.71	-	5.44	-
Theophylline	1.1	0.41	0.34	-	0.81	-
Lorazepam	1	0.09	0.46	-	4.15	-
Diazepam	0.53	0.02	0.21	-	6.3	-
Tolbutamide	0.38	0.05	0.21	-	3.49	-
Naproxen	0.19	0.01	0.18	-	9.75	-
Within 2-fold			50%	10%	60%	20%
Within 3-fold			80%	20%	60%	30%
Within 4-fold			90%	20%	60%	30%

Table 3. Predicted drug clearance rates in MPCCs as compared to suspension cultures created using the same donor (RTM). MPCCs were stabilized for 7 days prior to dosing with drugs for up to 7 days, while suspension hepatocytes were used immediately following thawing for up to 4 hours incubation with drugs. The '-' indicates that the drug did not turnover sufficiently in the model system to predict a clearance rate.

A

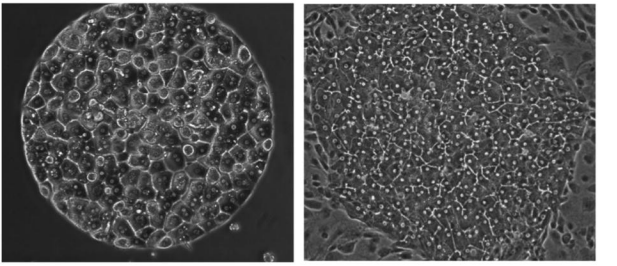

B

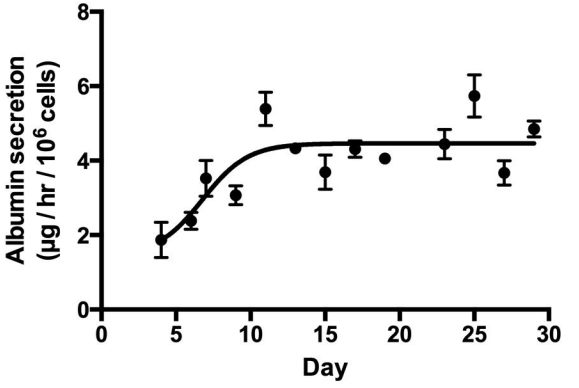
Albumin secretion
(μg / hr / 10^6 cells)
0
2
4
6
8
0
5
10
15
20
25
30
Day

C

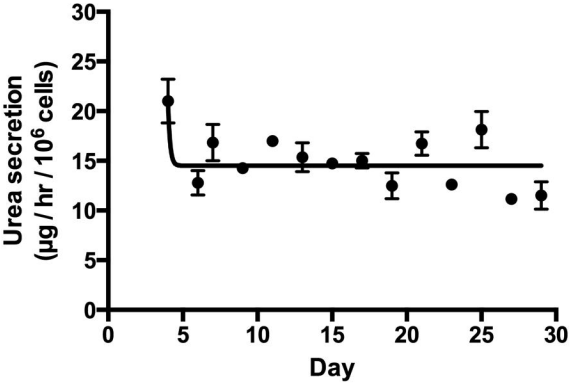
Urea secretion
(μg / hr / 10^6 cells)
0
5
10
15
20
25
30
0
5
10
15
20
25
30
Day

Figure 1

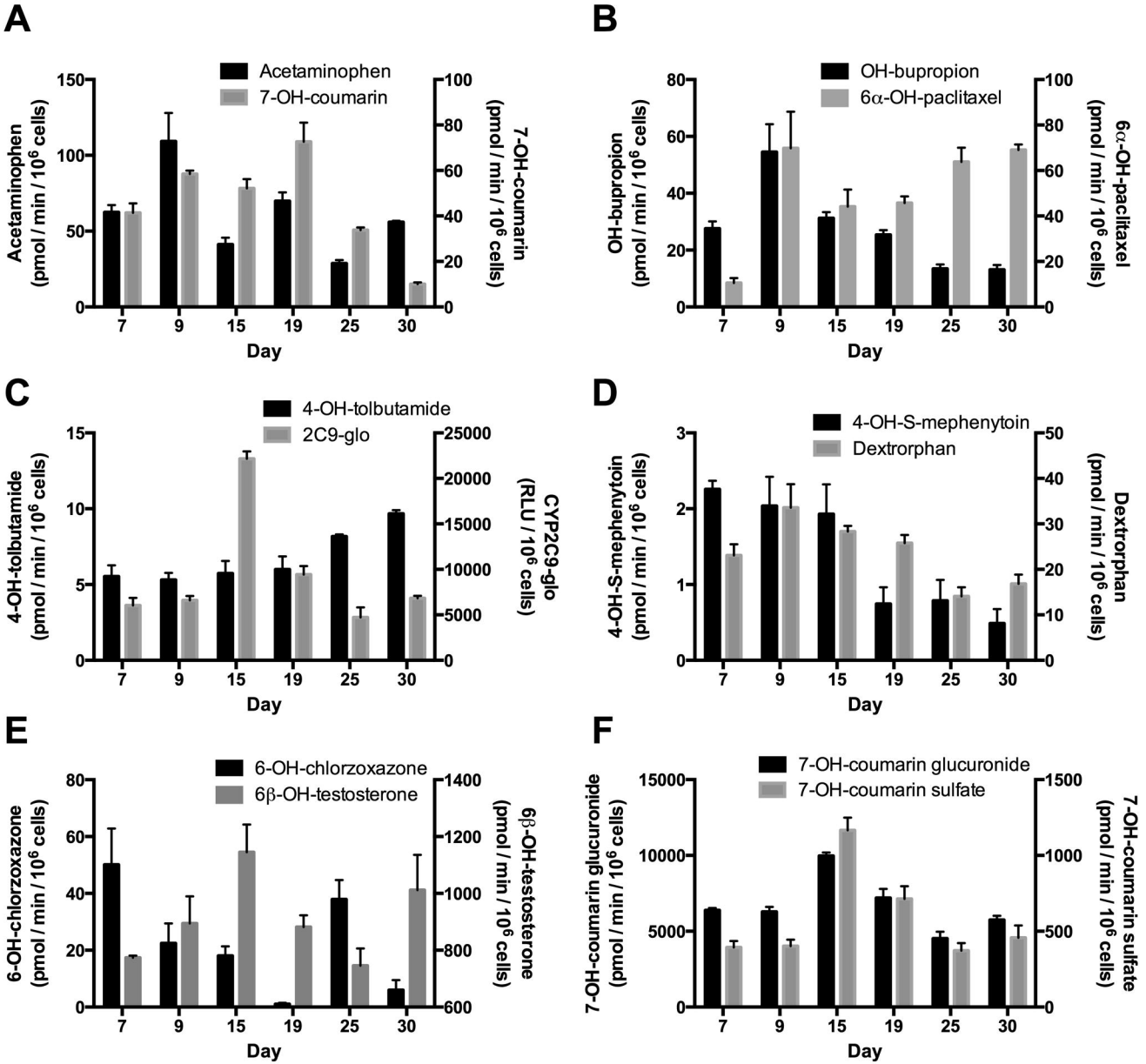
A
Acetaminophen
7-OH-coumarin
Acetaminophen (pmol / min / 10^6 cells)
7-OH-coumarin (pmol / min / 10^6 cells)
Day
B
OH-bupropion
6α-OH-paclitaxel
OH-bupropion (pmol / min / 10^6 cells)
6α-OH-paclitaxel (pmol / min / 10^6 cells)
Day
C
4-OH-tolbutamide
2C9-glo
4-OH-tolbutamide (pmol / min / 10^6 cells)
CYP2C9-glo (RLU / 10^6 cells)
Day
D
4-OH-S-mephenytoin
Dextrorphan
4-OH-S-mephenytoin (pmol / min / 10^6 cells)
Dextrorphan (pmol / min / 10^6 cells)
Day
E
6-OH-chlorzoxazone
6β-OH-testosterone
6-OH-chlorzoxazone (pmol / min / 10^6 cells)
6β-OH-testosterone (pmol / min / 10^6 cells)
Day
F
7-OH-coumarin glucuronide
7-OH-coumarin sulfate
7-OH-coumarin glucuronide (pmol / min / 10^6 cells)
7-OH-coumarin sulfate (pmol / min / 10^6 cells)
Day

Figure 2

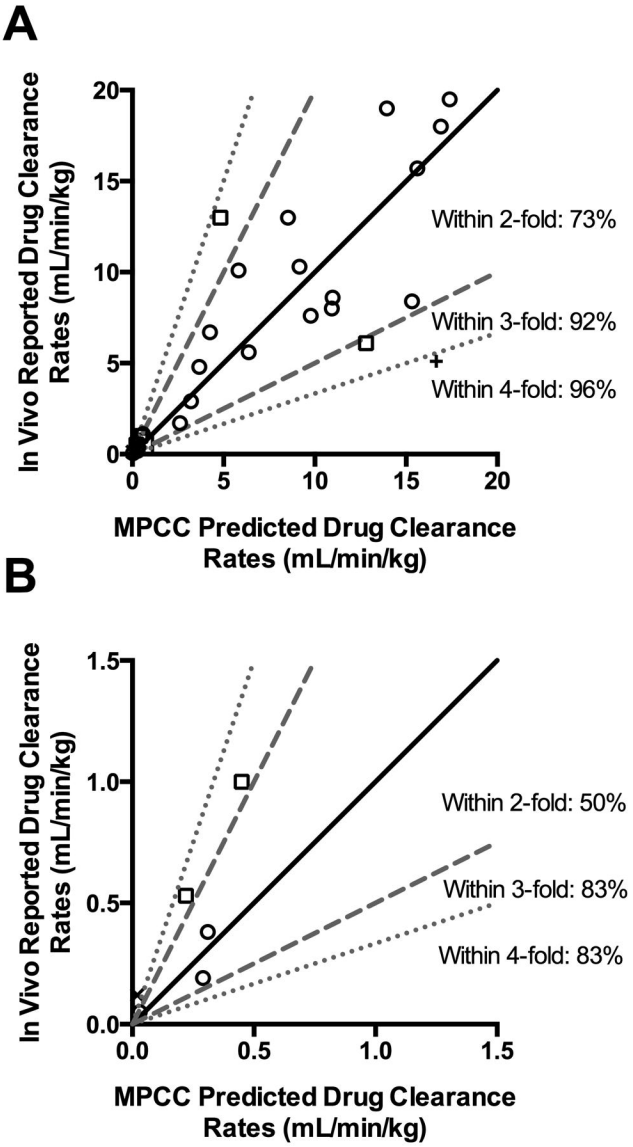
A
In Vivo Reported Drug Clearance Rates (mL/min/kg)
20
15
10
5
0
0
5
10
15
20
Within 2-fold: 73%
Within 3-fold: 92%
Within 4-fold: 96%
MPCC Predicted Drug Clearance Rates (mL/min/kg)
B
In Vivo Reported Drug Clearance Rates (mL/min/kg)
1.5
1.0
0.5
0.0
0.0
0.5
1.0
1.5
Within 2-fold: 50%
Within 3-fold: 83%
Within 4-fold: 83%
MPCC Predicted Drug Clearance Rates (mL/min/kg)

Figure 3

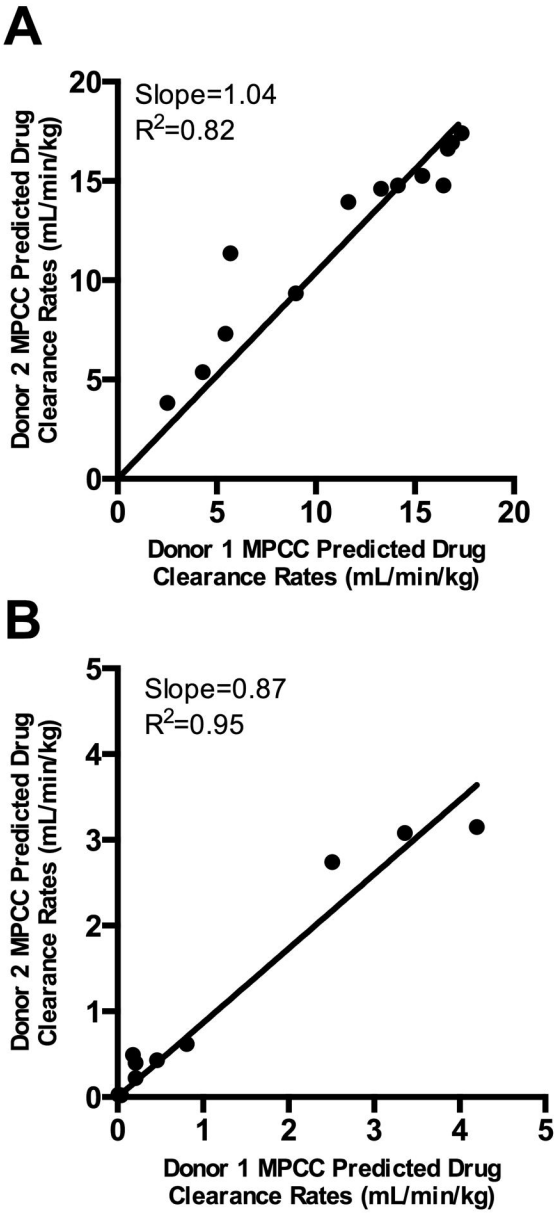
A
Slope=1.04
R2=0.82
Donor 2 MPCC Predicted Drug Clearance Rates (mL/min/kg)
Donor 1 MPCC Predicted Drug Clearance Rates (mL/min/kg)
0
5
10
15
20
B
Slope=0.87
R2=0.95
Donor 2 MPCC Predicted Drug Clearance Rates (mL/min/kg)
Donor 1 MPCC Predicted Drug Clearance Rates (mL/min/kg)
0
1
2
3
4
5

Figure 4

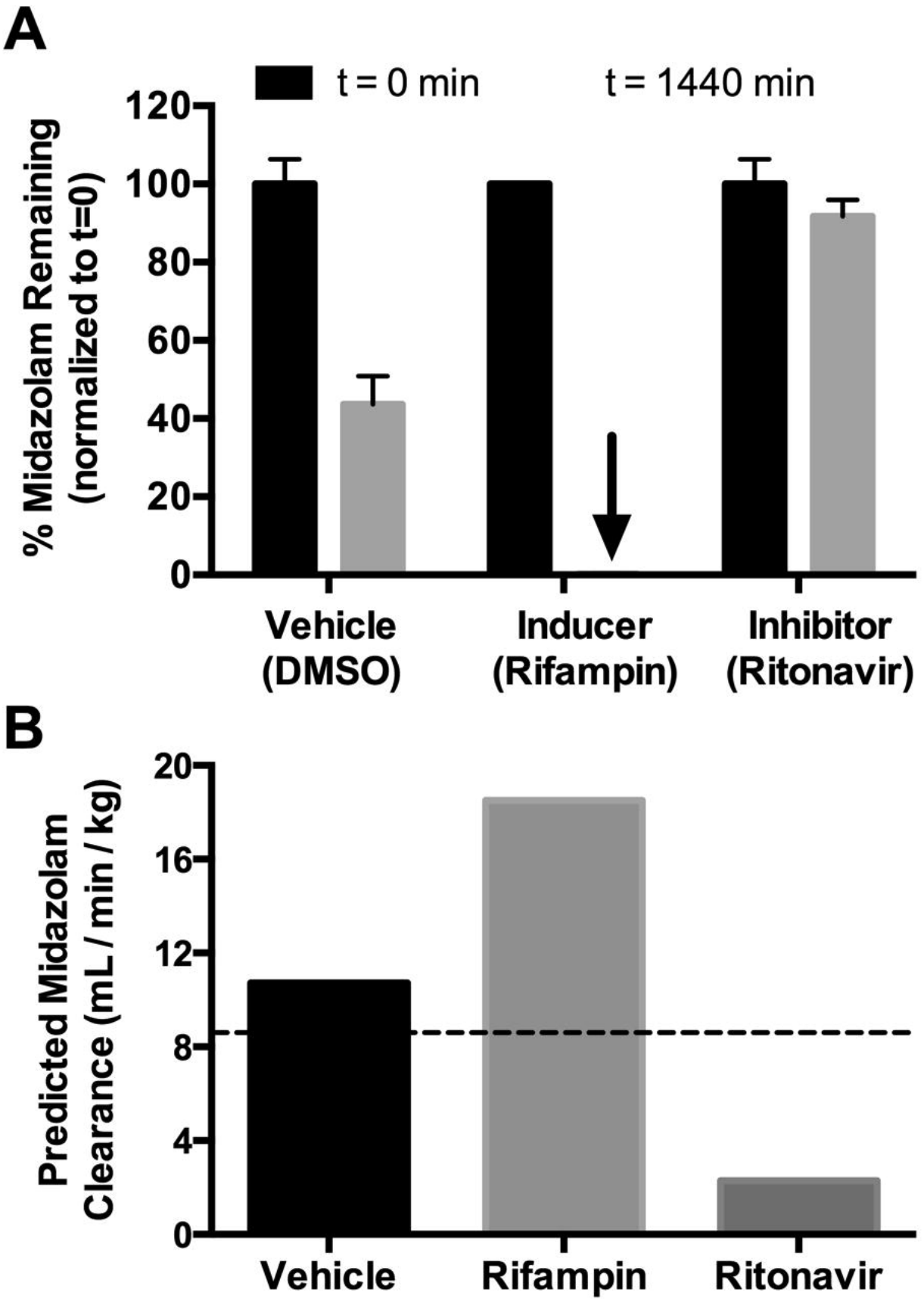
A
t = 0 min
t = 1440 min
% Midazolam Remaining
(normalized to t=0)
120
100
80
60
40
20
0
Vehicle
(DMSO)
Inducer
(Rifampin)
Inhibitor
(Ritonavir)
B
Predicted Midazolam
Clearance (mL / min / kg)
20
16
12
8
4
0
Vehicle
Rifampin
Ritonavir

Figure 5

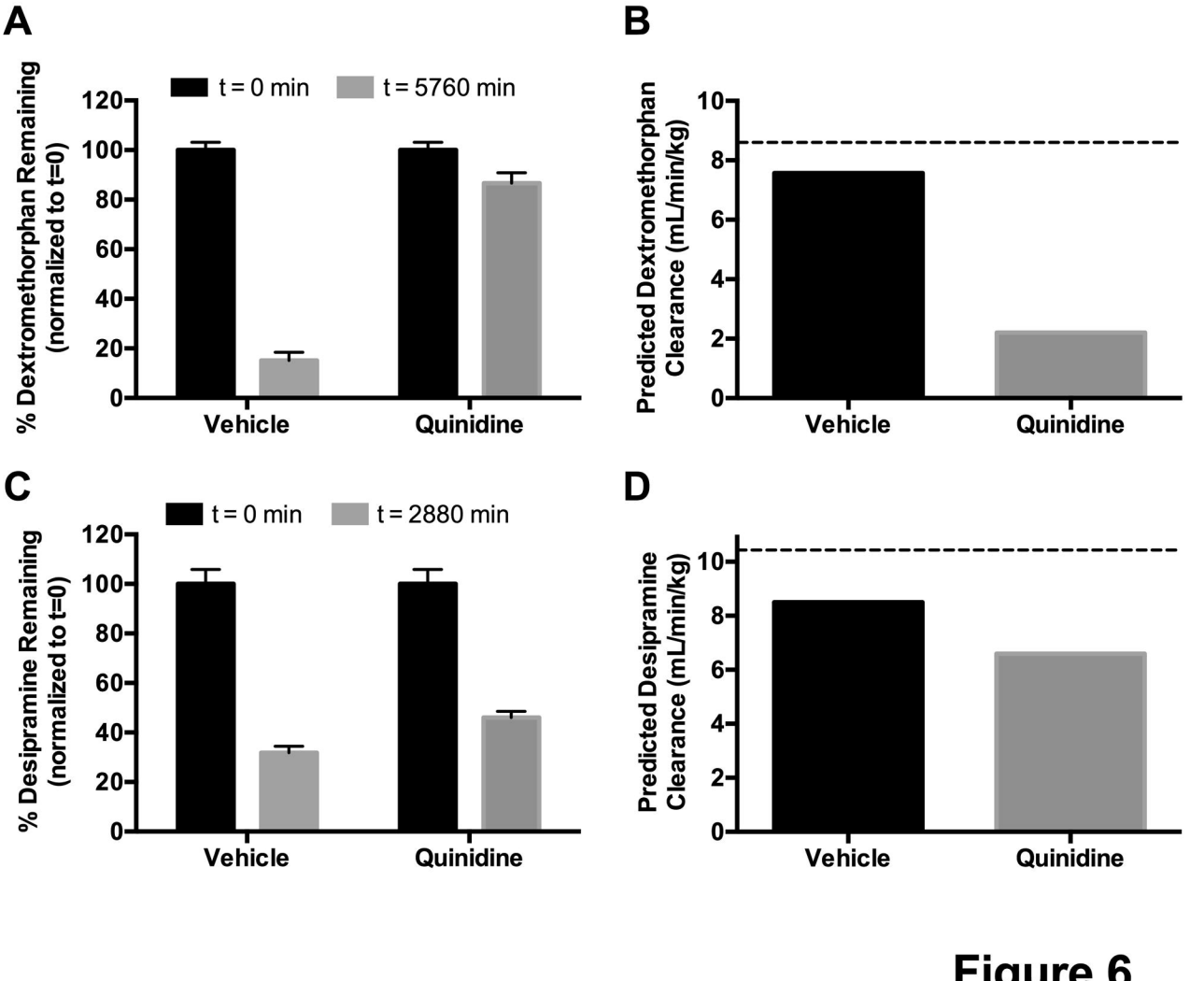
A
t = 0 min
t = 5760 min
% Dextromethorphan Remaining (normalized to t=0)
120
100
80
60
40
20
0
Vehicle
Quinidine
B
Predicted Dextromethorphan Clearance (mL/min/kg)
10
8
6
4
2
0
Vehicle
Quinidine
C
t = 0 min
t = 2880 min
% Desipramine Remaining (normalized to t=0)
120
100
80
60
40
20
0
Vehicle
Quinidine
D
Predicted Desipramine Clearance (mL/min/kg)
10
8
6
4
2
0
Vehicle
Quinidine

Figure 6